ARTICLE

OBC
www.rsc.org/obc

New pyrazolo[3,4-*b*]pyridones as selective A_1 adenosine receptor antagonists: synthesis, biological evaluation and molecular modelling studies

Paola Fossa,[a] Marco Pestarino,[a] Giulia Menozzi,*[a] Luisa Mosti,[a] Silvia Schenone,[a] Angelo Ranise,[a] Francesco Bondavalli,[a] M. Letizia Trincavelli,[b] Antonio Lucacchini[b] and Claudia Martini[b]

[a] *Dipartimento di Scienze Farmaceutiche, Università degli Studi di Genova, Viale Benedetto XV 3, 16132, Genova, Italy. E-mail: menozzi@unige.it; Fax: +39 010 3538358; Tel: +39 010 3538351*

[b] *Dipartimento di Psichiatria, Neurobiologia, Farmacologia e Biotecnologie, Università degli Studi di Pisa, Via Bonanno Pisano 6, 56126, Pisa, Italy; Fax: +39 050 2219609; Tel: +39 050 2219526*

Received 24th February 2005, Accepted 28th April 2005
First published as an Advance Article on the web 19th May 2005

A series of ethyl 4-amino-1-(2-chloro-2-phenylethyl)-6-oxo-6,7-dihydro-1*H*-pyrazolo[3,4-*b*]pyridine-5-carboxylates (**5a–j**) has been synthesized as potential A_1 adenosine receptor (A_1 AR) ligands. Binding affinities of the new compounds were determined for adenosine A_1, A_{2A} and A_3 receptors. Compounds **5b** and **5g** showed good affinity ($K_i = 299$ nM and 517 nM, respectively) and selectivity towards A_1 AR, whereas **5f** showed good affinity for A_{2A} AR ($K_i = 290$ nM), higher than towards A_1 AR ($K_i = 1000$ nM). The only arylamino derivative of the series **5j** displayed high affinity ($K_i = 4.6$ nM) and selectivity for A_3 AR. Molecular modelling and 3D-QSAR (CoMFA) studies carried out on the most active compounds gave further support to the pharmacological results.

Introduction

Adenosine is a powerful and widespread natural neuromodulator in the nervous system.[1] It is also an intermediate of the metabolic pathways responsible for adenine nucleotide salvage and recycling that are critical for the maintenance of ATP (itself an adenine nucleotide) levels in all types of cells, including neurones. Adenosine has numerous actions but, in particular, in the central nervous system it powerfully suppresses glutamate release from presynaptic terminals in hippocampus[2] and also directly hyperpolarises neurones *via* activation of G-protein coupled inwardly rectifying potassium (GIRK) channels at the postsynaptic site.[3] Its biological functions are exploited by activation of G-protein coupled receptors classified into A_1, A_{2A}, A_{2B} and A_3 subtypes. Adenosine receptors (ARs) from different species show 82–93% amino acid sequence homology, the only exception being the A_3 subtype, which exhibits 74% primary sequence homology between rat and human.[4]

In the last few years, much effort has been directed towards the synthesis of selective AR antagonists since they are attractive tools for pharmacological intervention in many pathophysiological conditions.[5] In particular, A_1 AR selective antagonists have been developed as antihypertensives and potassium-saving diuretics,[6] cognition enhancers[5] and useful therapeutics for the alleviation of the symptoms of Alzheimer's disease.[5,6] Among these, a wide variety of nitrogen-containing heterocycles have been synthesized as possible A_1 selective antagonists and pyrazolo[3,4-*b*]pyridine[7] and pyrazolo[3,4-*d*]pyrimidine[8] derivatives were found to be selective ligands with antagonistic activity for A_1 ARs.

In the course of our studies directed to obtain new non-classical adenosine ligands,[9,10] we synthesized a series of ethyl 4-amino-1-(2-chloro-2-phenylethyl)-1*H*-pyrazolo[3,4-*b*]pyridine-5-carboxylates **1** (see Fig. 1), some of which showed interesting affinity and antagonistic activity towards A_1 AR.[9] As a continuation of these studies we have then planned the synthesis of the pyrazolo[3,4-*b*]pyridone derivatives **5a–j**, analogues of **1**, in order to further explore structure–activity relationships in this class of compounds also. In parallel with the biological evaluation, a computational study with the theoretical model of A_1 AR, previously published by us,[11] has been performed to better understand the pharmacological results and to gain insight into the binding mode of some families of non-classical A_1 antagonists, in particular of the newly synthesized pyrazolo[3,4-*b*]pyridones. The results of this latest approach have been evaluated with a 3D-QSAR analysis, obtaining useful suggestions for the rational design of new derivatives.

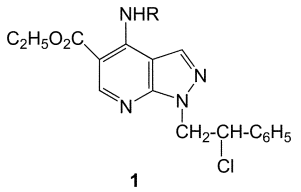

1

Fig. 1 Molecular formula of compounds **1**.

Results and discussion

Chemistry

The synthetic route to the target pyrazolo[3,4-*b*]pyridones **5a–j** is depicted in Scheme 1. Starting compound, namely ethyl 5-amino-1-(2-hydroxy-2-phenylethyl)-1*H*-pyrazole-4-carboxylate **2**, was prepared according to the procedure reported in a previous paper.[9] Condensation of **2** with diethyl malonate gave the cyclization to ethyl 4-hydroxy-1-(2-hydroxy-2-phenylethyl)-6-oxo-6,7-dihydro-1*H*-pyrazolo[3,4-*b*]pyridine-5-carboxylate **3**. Treatment of **3** with a mixture of thionyl chloride and dimethylformamide provided the dichloroderivative **4**. Finally, the aromatic displacement of the C4 chloro substituent of the intermediate **4** with various amines gave the pyrazolo[3,4-*b*]pyridones **5a–j**.

The nucleophilic substitution was performed under microwave irradiation (CEM Discovery system), to enhance yields and to reduce reaction times. Microwave technology, indeed, can

DOI: 10.1039/b502831k

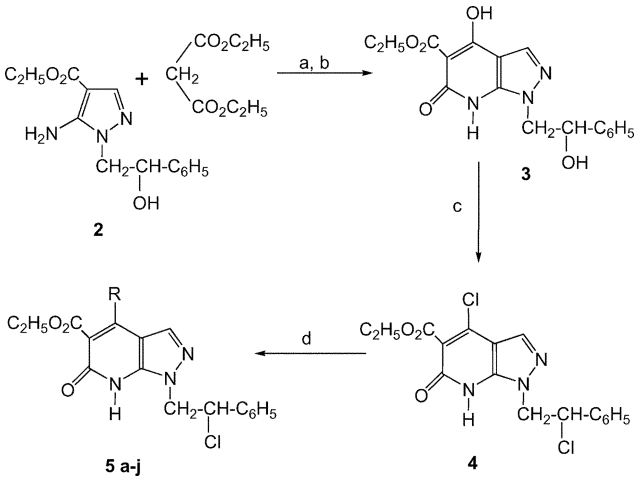

Scheme 1 *Compounds*: **5a**, R = $NH(CH_2)_2CH_3$; **5b**, R = $NHCH_2C_6H_5$; **5c**, R = $NH(CH_2)_2C_6H_5$; **5d**, R= $NHCH(CH_3)C_6H_5$; **5e**, R = $NH(CH_2)_2OC_2H_5$; **5f**, R = NH-cyclopropyl; **5g**, R = NH-cyclopentyl; **5h**, R = NH-cyclohexyl; **5i**, R = 1-pyrrolidinyl; **5j**, R = NHC_6H_5. *Reagents and conditions*: (a) EtONa, absolute ethanol, reflux, 6 h; (b) dil. HCl; (c) $SOCl_2$, DMFA, chloroform, reflux, 3 h; (d) method A: amine, CH_3COOH, dioxane, microwave irradiation, 10 min; method B: amine, chloroform, 60 °C, 2 h.

be successfully applied in many organic reactions[12] and, in particular, it was demonstrated to be useful in nucleophilic aromatic substitutions.[13] Compounds **5c**, **5f** and **5j** were also prepared by conventional procedure, to compare the yields obtained from the two methods. All the reactions were performed in closed vessels, but employing different solvents and experimental conditions. Microwave-assisted reactions were carried out in dioxane added with acetic acid, under irradiation at 300 W (final temperature 150 °C, pressure 35 psi), for 10 min. Following the conventional procedure, reactions were performed in chloroform, at the temperature of 60 °C, for 2 h. Experimental results confirmed that the conventional method, besides requiring a longer reaction time, gives lower yield, in comparison with the microwave-assisted technique (see Experimental).

Biological evaluation of compounds 5a–j

The biological activity of the compounds was tested by radioligand competition experiments.

The A_1, A_{2A} and A_3 AR binding affinities for compounds **5a–j** are expressed as K_i or the percentage of inhibition of binding (at 10 μM compound concentration) and are reported in Table 1.

The results of the binding tests of the newly synthesized derivatives showed various affinity levels towards A_1 or A_{2A} or A_3 ARs, in most cases with poor selectivity.

If we compare the results of the binding tests of the new pyrazolo[3,4-*b*]pyridone derivatives **5** with the data relevant to pyrazolo[3,4-*b*]pyridine analogues **1**,[9] we can notice, generally, a decrease in A_1 AR affinity and a rise in A_{2A} AR affinity. It should be remarked that compounds **5a**, **5d** and **5f** exhibited an A_{2A} AR affinity higher than A_1 AR affinity. Compounds **5b** and **5g** showed the highest affinity, with some selectivity, towards A_1 AR. The N^6-cyclopentyl substituent is actually known to induce high adenosine A_1 receptor affinity and selectivity.[14]

The cyclopropylamino substituent, on the contrary, gave an A_{2A} AR affinity higher than A_1 AR affinity (compound **5f**) in this series.

Only the anilino derivative **5j** exhibited high affinity and selectivity towards A_3 AR.

Structure–activity relationship (SAR) considerations

The biological results of the new pyrazolo-pyridones showed that the variation of the nature of the amino substituent at the C4 position significantly influenced the ARs affinity in the following ways: elongation, ramification, shortening of the benzyl chain of **5b**, the most active A_1 AR ligand of the series, gave derivatives **5c**, **5d** and **5j**, with a lower affinity towards both A_1 and A_{2A} ARs, in comparison with **5b**; a short alkyl or cycloalkyl substituent (*n*-propyl or cyclopropyl of compounds **5a** and **5f**, respectively) was associated with an A_{2A} affinity higher than A_1 AR affinity; in the case of cyclopropyl derivative **5f** a higher affinity towards both A_1 and A_{2A} ARs, together with a poor A_{2A} AR selectivity, was found; in comparison with the *n*-propyl derivative **5a**, the introduction of a longer alkoxyalkyl chain (**5e**) increased the affinity towards both A_1 and A_{2A} ARs, with loss of selectivity; enlargement of the aliphatic ring from three (**5f**) to five terms (**5g**) produced an increase in affinity and selectivity towards A_1 AR, while a further enlargement to six terms (**5h**) brought about a reduction in both A_1 and A_{2A} ARs affinity; substitution of a secondary amino group with a tertiary one (1-pyrrolidinyl derivative **5i**) maintained some affinity towards both A_1 and A_{2A} ARs, with loss of selectivity; the anilino group produced high affinity and selectivity towards A_3 AR.

Table 1 Affinity of **5a–j** derivatives towards bovine A_1, A_{2A} ARs and human A_3 ARs

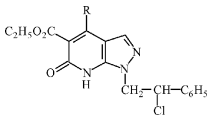

Compound	R	K_i/nM or inhibition (%)[a]		
		Bovine A_1[b]	Bovine A_{2A}[c]	Human A_3[d]
5a	$NH(CH_2)_2CH_3$	54%	2341	21%
5b	$NHCH_2C_6H_5$	299	2103	38%
5c	$NH(CH_2)_2C_6H_5$	40%	6%	13%
5d	$NHCH(CH_3)C_6H_5$	48%	1299	29%
5e	$NH(CH_2)_2OC_2H_5$	1285	1492	30%
5f	NH-cyclopropyl	1000	290	3663
5g	NH-cyclopentyl	517	2459	31%
5h	NH-cyclohexyl	2443	24%	16%
5i	1-Pyrrolidinyl	2173	2696	18%
5j	NHC_6H_5	46%	52%	4.6

[a] The K_i values are means ± SEM of three separate assays, each performed in triplicate. [b] Displacement of specific [^{3}H]DPCPX binding in bovine cortical membranes or percentage of inhibition of specific binding at 10 μM concentration. [c] Displacement of specific [^{3}H]CGS21680 binding in bovine striatal membranes or percentage of inhibition of specific binding at 10 μM concentration. [d] Displacement of specific [^{125}I] AB-MECA binding in CHO cell membranes or percentage of inhibition of specific binding at 1 μM concentration.

Molecular modelling studies

In order to further rationalize the biological results obtained, compounds displaying the most interesting activity on the A_1 AR, **5b** and **5g**, were docked by means of FlexX[15] into our A_1 AR virtual model.[11] In order to properly evaluate the validity of such a theoretical approach, in the absence of any structural data on the binding mode of any adenosine receptor ligand and its biological target, a data set of twelve selective A_1 AR antagonists, **14–16**, **35**, **46**, **56**, **64** and **67–71**, Table 2, representative for different chemical families, was docked into A_1 AR. The main molecular interactions between the A_1AR and compounds **14–16**, **35**, **46**, **56**, **64** and **67–71**, plus **5b** and **5g**, are presented in Table 3. According to our calculations, a binding area common to all the antagonists studied was defined. Compounds **5b** and **5g** were also accommodated here. In this area (Fig. 2 and Table 3), hydrogen bonding with residue Thr91 seems necessary for the interaction of any ligand with the receptor, while the affinity of the antagonist appears to be determined by additional H-bonds with residue His251, in agreement with results coming from site-directed mutagenesis experiments.[4] Near these hydrophilic interactions, hydrophobic interactions with three binding pockets, characterized by a different capacity of allocating hydrophobic portions of the ligands,[9] play a key-role in modulating the affinity of the antagonist with the biomolecule. According to our docking studies, pocket P1, defined by amino acid residues Ile67, Val 87, Leu88 and Thr91, is able to accept various substituents (R or R' on the molecular skeleton) even with a significant steric hindrance. Pocket P2, defined by residues Trp188, Leu250, His251 and Asp254, and pocket P3, defined by residues Ser94, Ile95, Leu98, Thr277 and Ser281, could accommodate only short alkyl or small cycloalkyl substituents without any further branching. On the basis of these binding simulations, the affinity of the antagonist towards the receptor is greatly determined by its ability to properly occupy all the three pockets at the same time.

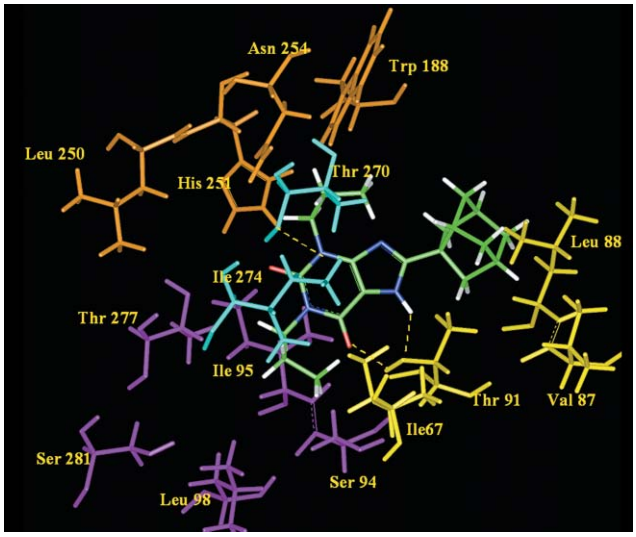

Fig. 2 Compound **15** (KW3902), coloured by atom type, docked into the binding site of A_1 AR. For clarity, only the most important residues are reported and labelled. The three hydrophobic pockets are coloured as follows: P1 in yellow, P2 in orange and P3 in magenta. Two residues not part of a pocket but important for the binding are coloured in cyan.

In *tandem* with our molecular docking studies, a quantitative evaluation of the structure–activity relationships inside A_1 AR antagonists has been performed through a comparative molecular field analysis (CoMFA)[16] study, on compounds **6–71** (Table 2). The CoMFA method is widely used as 3D-QSAR technique to relate the biological activity of a series of molecules with their steric and electrostatic fields sampled at several grid points around the molecule by means of a suitable probe, usually an sp^3 carbon atom with a charge of +1. Partial Least Squares (PLS) is used as the regression method to develop the relationship between steric and electrostatic potentials and biological activity. The graphical representation of CoMFA model, in the form of coefficient isocontour maps, efficiently locates the regions where the variation in steric and electrostatic properties of different molecules in a data set is correlated with the variation of biological activity. CoMFA isocontour maps may thus provide useful indications to develop sound working hypothesis on the nature of putative ligand–macromolecule interactions.

In the present work, CoMFA models were developed using a common structure alignment derived from the superimposition of structures **14–16**, **35**, **46**, **56**, **64** and **67–71** as derived from docking studies. Results for the best model obtained are reported in Table 4. The model exhibited a cross-validated r^2 (r^2_{cv}) of 0.540 with cancellation groups validation procedure. A non-cross-validated r^2 (r^2_{ncv}) of 0.937 was obtained.

In addition, almost equal contributions were observed for steric (52%) and electrostatic (48%) fields, represented in Fig. 3 as 3D contour plots, suggesting a balanced model with slightly prevalent steric effects.

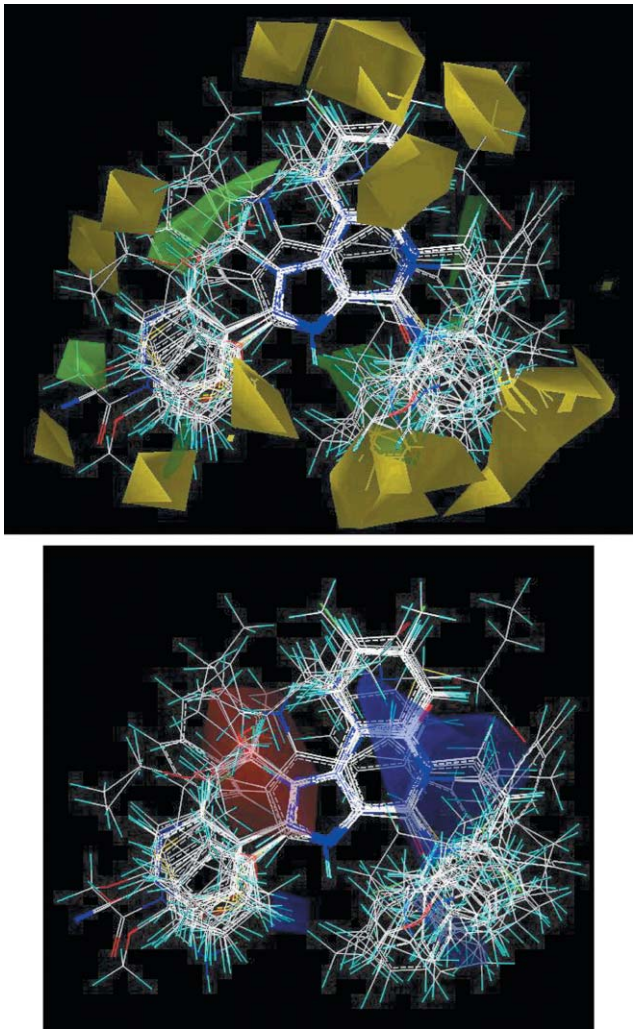

Fig. 3 CoMFA steric and electrostatic contour maps. Yellow denotes regions where steric bulk is detrimental to activity and green denotes regions where steric bulk enhances activity. Red denotes regions where positive charge is detrimental to activity and blue denotes region where positive charge enhances activity. The superimposed antagonists **6–71** are also shown.

The steric contour map (Fig. 3) showed yellow (steric unfavourable interaction) polyhedra differently delimiting the

Table 2 Molecular formulas of compounds **6–71**

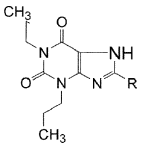

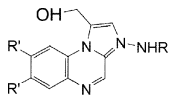

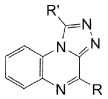

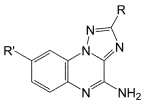

Comp.	R	pK_i	Comp.	R	R′	pK_i	Comp.	R	R′	pK_i	Comp.	R	R′	pK_i
6	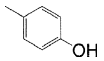	0.2	**17**	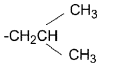	H	−1.82	**25**		$-CH_2CH_3$	−2.42	**37**		H	−1.77
7		−0.51	**18**	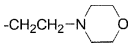	H	−1.34	**26**		H	−2.26	**38**		Cl	−1.70
8		−0.31	**19**	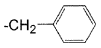	CH_3	−1.64	**27**		$-CH_2CH_3$	−1.44	**39**		CH_3	−1.58
9	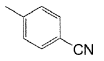	−0.66	**20**	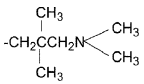	CH_3	−1.51	**28**		$-CH_2CH_3$	−2.79	**40**		Cl	−2.18
10		0.52	**21**	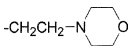	CH_3	−1.36	**29**		$-CH_2CH_3$	−1.77	**41**		Cl	−1.55
11	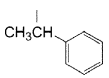	−1.77	**22**		Cl	−1.96	**30**		$-CH_2CH_3$	−2.36	**42**		H	−1.48
12		−0.51	**23**	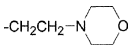	Cl	−1.85	**31**		$-CH_2CH_3$	−1.90	**43**		Cl	−1.48
13		−1.04	**24**	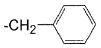	Cl	−1.80	**32**		$-CH_2CH_2CH_3$	−1.56	**44**		Cl	−1.36
14		0.33					**33**		$-CH_2CH_2CH_2CH_3$	−1.74	**45**		Cl	−1.08
15		0.72					**34**		$-CH_2CH_3$	−1.64	**46**		Cl	−1.11
16		−0.11					**35**		CF_3	−0.90				
							36		CH_3	−0.86				

Table 2 *(Contd.)*

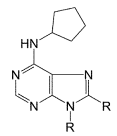
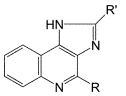
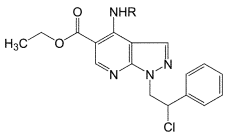

Comp.	R	R′	pK_i	Comp.	R	R′	pK_i	Comp.	R	pK_i	Comp.		pK_i
47	Br	CH_3	−1.64	**57**		H	−1.64	**65**		−2.05	**68**	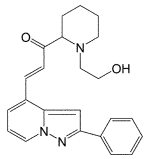	0.31
48		CH_3	−1.60	**58**			−2.66	**66**	$–CH_2CH_2CH_3$	−2.00	**69**	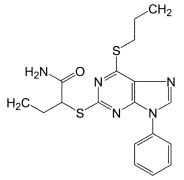	−1.47
49	Br		−3.09	**59**			−2.37	**67**	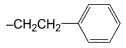	−1.70	**70**	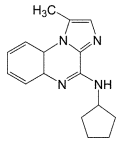	−0.90
50	Br	$–CH_2CH_2CH_3$	−1.52	**60**	NH_2		−2.43				**71**	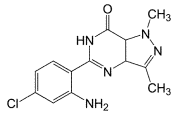	−2.34
51	$–SCH_2CH_3$	CH_3	−2.35	**61**			−1.58						
52	Br	$–CH_2CH{=}CH_3$	−1.55	**62**	NH_2		−1.54						
53	$–OCH_2CH_3$	CH_3	−2.03	**63**	NH_2	H	−3.20						
54	Br	H	−2.96	**64**			−1.00						
55	$–OCH_3$	CH_3	−2.08										
56	H	CH_3	−2.73										

Table 3 Main protein–ligand interactions as displayed by the best docking orientation for each inhibitor

Compound	Amino acid residues involved in H-bonds	Amino acid residues involved lipophilic interactions
14	Thr91, Ser94, His251	Ile67, Leu88, Ile95, Leu250, Ala273, Ile274
15	Thr91, Ser94, His251	Ile67, Leu88, Ile95, Ile274
16	Thr91, Ser94, His251	Leu88, Ile95, Leu250, Ile274
35	Thr91, His251	Ile67, Ile95, Ile274
46	Thr91, His251	Ile67, Val87, Ile95
56	Thr91, His251	Ile274
64	Thr91, His251	Ile95, Ile274
67	Thr91	Ile95, Ala273, Ile274
68	Thr91, His251	Leu88, Ala273, Ile274
69	Thr91, His251	Ile67, Leu88, Ile95, Ile274
70	Thr91	Ile67, Ile95, Ile274
71	Thr91, Trp188	Ile274
5b	Thr91, Ser94	Ile67, Ile95
5g	Thr91	Ile67, Ile95

Table 4 Summary of CoMFA–PLS results

No. of compounds	65
Opt. no. of components	5
Cross-validated r^2	0.540
Std error of estimate	0.229
Non-cross-validated r^2	0.937
F Values	141.867
Steric contribution	0.510
Electrostatic contribution	0.490
Std dev.	0.014
R^2bs	0.960

borders of the three pockets P1, P2 and P3. In agreement with the above reported docking studies, P1 is not strictly limited in size, while P2 and P3 are more conditioned by surrounding yellow regions. Some green (steric favourable interaction) polyhedra in correspondence to one side of P2 and P3 pockets defined spatial regions where a steric interaction between the ligand and the receptor would enhance the strength of the binding. On the basis of these findings, in the evaluation of steric contour maps of all the newly synthesized compounds **5**, derivatives **5b** and **5g** were the only ones able to occupy green regions avoiding the occupancy of any yellow portion. On the contrary, for all other compounds unfavourable steric interactions were observed within the CoMFA model. The electrostatic contour map, shown in Fig. 3, defined a blue region between P1 and P2 where the presence of positive charges enhances activity (electrostatic favourable interaction). This region corresponds mainly to tertiary heterocyclic nitrogen in the antagonist molecule. A small red region (electrostatic unfavourable interaction) where the presence of positive charges is detrimental for activity was instead defined at the border between P2 and P3 pockets. Almost all of the studied ligands with their polar substituents or polar groups did not occupy this area. According to these data, compounds **5**, characterized by a pyrazolo [3,4-*b*]pyridone nucleus, showed a slightly unfavourable electrostatic interaction with the counter part, positioning the carbonyl group in C-6 at the borderline of the red region. On the contrary, analogues **1**,[9] characterized by a pyrazolo [3,4-*b*]pyridine core, do not present any unfavourable electrostatic interaction with the counterpart. Thus, our calculations, as a further support to biological data, in the case of **5b** and **5g** suggest that the enhancement of activity due to favourable steric interactions is only slightly reduced by an unfavourable electrostatic interaction. For all others compounds **5** the sum of two detrimental contributions (mostly steric and only partially electrostatic) could justify the low affinity values experimentally determined towards A_1 AR.

Conclusions

In this report, we described the synthesis of a series of pyrazolo[3,4-*b*]pyridones **5a–j**, having the same pharmacophore at N^1 than pyrazolo[3,4-*b*]pyridine derivatives **1**[9] previously synthesized by us and endowed with a noteworthy A_1 AR antagonistic activity. Many of the newly synthesized compounds showed an interesting affinity towards A_1 and A_{2A} ARs, but poor selectivity. Compounds **5b** and **5g** turned out to be A_1 AR antagonists with good affinity (K_i = 299 and 517 nM, respectively) but a fair selectivity. Compound **5f**, on the contrary, showed good affinity towards A_{2A} AR (K_i = 290 nM) and **5j** exhibited high affinity (K_i = 4.6 nM) and selectivity towards A_3 AR. In conclusion, the biological data proved that the substitution of the pyridine ring in the structure of compounds **1** with the pyridone nucleus is not profitable for the A_1 AR antagonistic activity and selectivity. Unexpectedly, the introduction of an anilino group on the C4 position of the pyrazolopyridone scaffold (**5j**) provided high A_3 AR affinity and selectivity. Molecular modelling studies on A1 AR fully support and contribute to explain the experimental results obtained on A_1 AR. In particular, the coordinated use of CoMFA and docking approaches has lead to a significant and complementary insight into the complex biological interactions between antagonist and A_1 receptor. Helpful suggestions for the synthesis of new and more potent antagonists in the class of pyrazolo[3,4-*b*]pyridines will be derived from the CoMFA model.

Experimental

Chemistry protocols

All chemicals and solvents used were commercially available and of analytical grade or were prepared according to the procedure described in the literature.[9] All of the microwave-assisted reactions were performed in a CEM Discover system (CEM Corporation). All compounds were tested for purity by thin-layer chromatography (TLC) on silica gel plates (60 F_{254}, Merck; ethyl acetate–petroleum ether 1 : 1 as eluant), visualizing with ultraviolet light. Melting points were determined with a Fisher–Johns apparatus and are uncorrected. IR spectra were registered on a Perkin-Elmer 398 spectrophotometer and are expressed in cm^{-1}. ^1H NMR spectra were registered on a Varian Gemini 200 (200 MHz) spectrometer; chemical shifts are reported as δ values (ppm) relative to TMS as internal standard; coupling constants (J) are expressed in Hertz (Hz). The following NMR abbreviations are used: br (broad), s (singlet), d (doublet), t (triplet), q (quartet), m (multiplet) and ex (exchangeable with D_2O). Microanalyses for C, H, N were performed using a Carlo Erba Elemental Analyzer Model EA 1110 and results agree within ±0.4% with calculated values

Ethyl 4-hydroxy-1-(2-hydroxy-2-phenylethyl)-6-oxo-6,7-dihydro-1*H*-pyrazolo[3,4-*b*]pyridine-5-carboxylate 3. Diethyl malonate (9.61 g, 60 mmol) was slowly added to a solution of sodium ethoxide, prepared from sodium (2.07 g, 90 mmol) in absolute

ethanol (80 cm^3). After stirring at rt for 15 min, ethyl 5-amino-1-(2-hydroxy-2-phenylethyl)-1*H*-pyrazole-4-carboxylate **2** (8.26 g, 30 mmol) was added and the mixture obtained was refluxed for 6 h. After cooling, the reaction mixture was concentrated under a reduced pressure to half volume, diluted with water (100 cm^3), cooled in an ice bath and acidified to pH = 5 with diluted HCl (6 N and 1 N, successively). The white solid which separated was filtered and dried for 3 h in a vacuum oven at 100 °C. Recrystallization from glacial acetic acid afforded the title compound **3** (5.7 g, 55%); mp 188–190 °C (dec); (found: C, 59.43; H, 4.98; N, 12.31%. $C_{17}H_{17}N_3O_5$ requires C, 59.47; H, 4.99; N, 12.24%); ν_{max} (KBr)/cm^{-1} 3526, 1661, 1640 and 1615. δ_H (200 MHz; DMSO-d_6; Me_4Si): 1.30 (3 H, t, *J* 7.0, CH_2CH_3), 4.31 (2 H, q, *J* 7.0, CH_2CH_3), 4.1–4.6 (2 H, m, CH_2N), 4.95–5.05 (1 H, m, CHOH), 5.60 (1 H, br s, OH, ex), 7.2–7.6 (5 H, m, Ph), 7.99 (1 H, s, 3-H), 11.95 (1 H, s, 4-OH, ex), 13.45 (1 H, s, NH, ex).

Ethyl 4-chloro-1-(2-chloro-2-phenylethyl)-6-oxo-6,7-dihydro-1*H*-pyrazolo[3,4-*b*]pyridine-5-carboxylate 4. Ethyl 4-hydroxy-1-(2-hydroxy-2-phenylethyl)-6-oxo-6,7-dihydro-1*H*-pyrazolo-[3,4-*b*]-pyridine-5-carboxylate **3** (3.43 g, 10 mmol) was dissolved in a mixture of thionyl chloride (7.3 cm^3, 100 mmol), dimethylformamide (1.1 cm^3, 14 mmol) and chloroform (40 cm^3). The mixture was refluxed for 3 h, cooled and evaporated to dryness *in vacuo*. The residue was dissolved in chloroform (50 cm^3); this solution was washed twice with water (2 × 15 cm^3), dried by magnesium sulfate and evaporated *in vacuo*. The solid residue was purified by recrystallization from ethyl acetate to yield the title compound **4** as a white solid (2.05 g, 54%); mp 165–168 °C (dec); (found: C, 53.71; H, 4.20; N, 11.03%. $C_{17}H_{15}Cl_2N_3O_3$ requires C, 53.70; H, 3.98; N, 11.05%); ν_{max} ($CHCl_3$)/cm^{-1} 1732, 1642, 1611 and 1573. δ_H (200 MHz; $CDCl_3$; Me_4Si): 1.43 (3H, t, *J* 7.0, CH_2CH_3), 4.47 (2 H, q, *J* 7.0, CH_2CH_3), 4.65–4.80 and 4.95–5.10 (2 H, 2 dd, CH_2N), 5.45–5.55 (1 H, m, CHCl), 7.25–7.55 (5 H, m, Ph), 8.02 (1 H, s, 3-H), ~13.25 (1 H, very br s, NH, ex).

Method A: general procedure for the preparation of pyrazolo-[3,4-*b*]pyridones 5a–j. Representative preparation of ethyl 1-(2-chloro-2-phenylethyl)-6-oxo-4-propylamino-6,7-dihydro-1*H*-pyrazolo[3,4-*b*]pyridine-5-carboxylate 5a. A mixture of ethyl 4-chloro-1-(2-chloro-2-phenylethyl)-6-oxo-6,7-dihydro-1*H*-pyrazolo[3,4-*b*]pyridine-5-carboxylate **4** (0.5 g, 1.3 mmol), propylamine (0.12 g, 2 mmol), glacial acetic acid (0.12 g, 2 mmol) and dioxane (10 cm^3) in a closed vessel was exposed to microwave irradiation (power 300 W; final temperature 150 °C; pressure 35 psi) for 10 min. After cooling, the mixture was diluted with chloroform (50 cm^3), washed in succession with water (20 cm^3), saturated sodium carbonate solution (10 cm^3) and water (20 cm^3), dried by magnesium sulfate and evaporated *in vacuo*. The solid residue was recrystallized from 95% ethanol to yield the title compound **5a** as a white solid (0.44 g, 85%); mp 200–202 °C; (found: C, 59.33; H, 5.68; N, 13.84%. $C_{20}H_{23}ClN_4O_3$ requires C, 59.62; H, 5.75; N, 13.91%); ν_{max} ($CHCl_3$)/cm^{-1} 3403, 1643, 1611 and 1586. δ_H (200 MHz; $CDCl_3$; Me_4Si): 1.15 (3H, t, *J* 7.6, $NHCH_2CH_2CH_3$), 1.46 (3H, t, *J* 7.0, CH_2CH_3), 1.86 (2 H, sextet, *J* 7.2, $NHCH_2CH_2CH_3$), 3.5–3.7 (2 H, m, $NHCH_2CH_2CH_3$), 4.48 (2 H, q, *J* 7.0, CH_2CH_3), 4.65–4.80 and 4.95–5.10 (2 H, 2 dd, CH_2N), 5.50–5.65 (1 H, m, CHCl), 7.25–7.55 (5 H, m, Ph), 7.96 (1 H, s, 3-H), ~8.7 (1 H, very br s, NH, ex).

Ethyl 4-(benzylamino)-1-(2-chloro-2-phenylethyl)-6-oxo-6,7-dihydro-1*H*-pyrazolo[3,4-*b*]pyridine-5-carboxylate 5b. As described for **5a**, from **4** and benzylamine (0.21 g, 2 mmol). Recrystallization from 95% ethanol gave **5b** as a white solid (0.51 g, 86%); mp 174–176 °C; (found: C, 64.07; H, 5.12; N, 12.44%. $C_{24}H_{23}ClN_4O_3$ requires C, 63.93; H, 5.14; N, 12.42%); ν_{max} ($CHCl_3$)/cm^{-1} 3395, 1644, 1611 and 1583. δ_H (200 MHz; $CDCl_3$; Me_4Si): 1.20 (3 H, t, *J* 7.0, CH_2CH_3), 4.35 (2 H, q, *J* 7.0, CH_2CH_3), 4.65–4.80 and 4.90–5.10 (2 H, 2 dd, CH_2N), 4.84 (2 H, d, *J* 4.8, CH_2Ph), 5.50–5.65 (1 H, m, CHCl), 7.25–7.60 (10 H, m, 2 Ph), 7.95 (1 H, s, 3-H), ~8.9 (1 H, very br s, NH, ex), ~12.80 (1 H, very br s, NH, ex).

Ethyl 1-(2-chloro-2-phenylethyl)-6-oxo-4-(2-phenylethyl)amino-6,7-dihydro-1*H*-pyrazolo[3,4-*b*]pyridine-5-carboxylate 5c. As described for **5a**, from **4** and 2-phenylethylamine (0.24 g, 2 mmol). Recrystallization from 95% ethanol gave **5c** as a white solid (0.51 g, 85%); mp 183–185 °C; (found: C, 64.54; H, 5.46; N, 11.98%. $C_{25}H_{25}ClN_4O_3$ requires C, 64.58; H, 5.42; N, 12.05%); ν_{max} ($CHCl_3$)/cm^{-1} 3396, 1644, 1610 and 1585. δ_H (200 MHz; $CDCl_3$; Me_4Si): 1.24 (3 H, t, *J* 7.0, CH_2CH_3), 3.13 (2 H, t, *J* 7.0, $NHCH_2CH_2Ph$), 3.98 (2 H, q, *J* 7.0 Hz, $NHCH_2CH_2Ph$), 4.33 (2 H, q, *J* 7.0, CH_2CH_3), 4.65–4.80 and 4.90–5.10 (2 H, 2 dd, CH_2N), 5.50–5.65 (1 H, m, CHCl), 7.20–7.60 (10 H, m, 2 Ph), 7.99 (1 H, s, 3-H), ~8.40 (1 H, very br s, NH, ex), ~12.80 (1 H, very br s, NH, ex).

Ethyl 1-(2-chloro-2-phenylethyl)-6-oxo-4-(1-phenylethyl)amino-6,7-dihydro-1*H*-pyrazolo[3,4-*b*]pyridine-5-carboxylate 5d. As described for **5a**, from **4** and 1-phenylethylamine (0.24 g, 2 mmol). Recrystallization from 95% ethanol gave **5d** as a white solid (0.42 g, 70%); mp 186–187 °C; (found: C, 64.29; H, 5.52; N, 11.94%. $C_{25}H_{25}ClN_4O_3$ requires C, 64.58; H, 5.42; N, 12.05%); ν_{max} ($CHCl_3$)/cm^{-1} 3395, 1644, 1613 and 1582. δ_H (200 MHz; $CDCl_3$; Me_4Si): 1.42 (3 H, t, *J* 7.0, CH_2CH_3), 1.73 (3 H, d, *J* 6.8, $NHCH(Ph)CH_3$), 4.48 (2 H, q, *J* 7.0, CH_2CH_3), 4.60–5.00 (2 H, m, CH_2N), 5.16 (1 H, quintet, *J* 6.8, $NHCH(Ph)CH_3$), 5.40–5.55 (1 H, m, CHCl), 7.25–7.50 (10 H, m, 2 Ph), 7.67 (1 H, s, 3-H), ~9.18 (1 H, very br s, NH, ex).

Ethyl 1-(2-chloro-2-phenylethyl)-4-(2-ethoxyethyl)amino-6-oxo-6,7-dihydro-1*H*-pyrazolo[3,4-*b*]pyridine-5-carboxylate 5e. As described for **5a**, from **4** and 2-ethoxyethylamine (0.18 g, 2 mmol). Recrystallization from 95% ethanol gave **5e** as a white solid (0.44 g, 80%); mp 154–155 °C; (found: C, 59.98; H, 6.21; N, 13.31%. $C_{21}H_{25}ClN_4O_4$ requires C, 59.93; H, 5.99; N, 13.31%); ν_{max} ($CHCl_3$)/cm^{-1} 3393, 1644, 1609 and 1586. δ_H (200 MHz; $CDCl_3$; Me_4Si): 1.29 (3H, t, *J* 7.0, $NHCH_2CH_2OCH_2CH_3$), 1.48 (3 H, t, *J* 7.0, CH_2CH_3), 3.63 (2 H, q, *J* 7.0, $NHCH_2CH_2OCH_2CH_3$), 3.70–4.00 (4 H, m, $NHCH_2CH_2OCH_2CH_3$), 4.51 (2 H, q, *J* 7.0, CH_2CH_3), 4.65–4.80 and 4.90–5.05 (2 H, 2 dd, CH_2N), 5.50–5.65 (1 H, m, CHCl), 7.25–7.60 (5 H, m, Ph), 7.95 (1 H, s, 3-H), ~8.65 (1 H, very br s, NH, ex), ~12.80 (1 H, very br s, NH, ex).

Ethyl 1-(2-chloro-2-phenylethyl)-4-cyclopropylamino-6-oxo-6,7-dihydro-1*H*-pyrazolo[3,4-*b*]pyridine-5-carboxylate 5f. As described for **5a**, from **4** and cyclopropylamine (0.11 g, 2 mmol). Recrystallization from 95% ethanol gave **5f** as a white solid (0.39 g, 75%); mp 206–208 °C; (found: C, 59.99; H, 5.26; N, 13.80%. $C_{20}H_{21}ClN_4O_3$ requires C, 59.92; H, 5.28; N, 13.98%); ν_{max} ($CHCl_3$)/cm^{-1} 3407, 1644, 1613 and 1585. δ_H (200 MHz; $CDCl_3$; Me_4Si): 0.60–0.75 and 0.95–1.10 (4 H, 2 m, CH_2CH_2), 1.25 (3 H, t, *J* 7.0, CH_2CH_3), 2.95–3.10 (1 H, m, CH cyclopropyl), 4.23 (2 H, q, *J* 7.0, CH_2CH_3), 4.50–4.70 and 4.95–5.15 (2 H, 2 dd, CH_2N), 5.50–5.65 (1 H, m, CHCl), 7.35–7.70 (5 H, m, Ph), 8.32 (1 H, s, 3-H), ~9.60 (1 H, very br s, NH, ex) and ~11.70 (1 H, very br s, NH, ex).

Ethyl 1-(2-chloro-2-phenylethyl)-4-cyclopentylamino-6-oxo-6,7-dihydro-1*H*-pyrazolo[3,4-*b*]pyridine-5-carboxylate 5g. As described for **5a**, from **4** and cyclopentylamine (0.17 g, 2 mmol). Recrystallization from 95% ethanol gave **5g** as a white solid (0.40 g, 71%); mp 192–193 °C; (found: C, 61.51; H, 5.87; N, 13.02%. $C_{22}H_{25}ClN_4O_3$ requires C, 61.61; H, 5.87; N, 13.06%); ν_{max} ($CHCl_3$)/cm^{-1} 3396, 1644, 1610 and 1584. δ_H (200 MHz; $CDCl_3$; Me_4Si): 1.46 (3 H, t, *J* 7.2, CH_2CH_3), 1.65–1.90 (4 H, m, CH_2CH_2), 2.10–2.25 (4 H, m, CH_2CHCH_2), 4.30–4.50 (1 H, m, cyclopropyl CH), 4.47 (2 H, q, *J* 7.0, CH_2CH_3), 4.65–4.80 and 4.95–5.10 (2 H, 2 dd, CH_2N), 5.50–5.60 (1 H, m, CHCl),

7.25–7.55 (5 H, m, Ph), 7.96 (1 H, s, 3-H), ~8.75 (1 H, very br s, NH, ex).

Ethyl 1-(2-chloro-2-phenylethyl)-4-cycloexylamino-6-oxo-6,7-dihydro-1*H*-pyrazolo[3,4-*b*]pyridine-5-carboxylate 5h. As described for **5a**, from **4** and cyclohexylamine (0.2 g, 2 mmol). Recrystallization from 95% ethanol gave **5h** as a white solid (0.46 g, 81%); mp 233–234 °C; (found: C, 62.67; H, 6.11; N, 12.58%. $C_{23}H_{27}ClN_4O_3$ requires C, 62.37; H, 6.14; N, 12.65%); ν_{max} ($CHCl_3$)/cm^{-1} 3391, 1634, 1604 and 1584. δ_H (200 MHz; $CDCl_3$; Me_4Si): 1.47 (3 H, t, *J* 7.0, CH_2CH_3), 1.30–1.95 (8 H, m, 4 CH_2 cyclohexyl), 2.10–2.25 (2 H, m, CH_2 cyclohexyl), 3.80–3.95 (1 H, m, CH), 4.49 (2 H, q, *J* 7.0, CH_2CH_3), 4.65–4.75 and 4.95–5.10 (2 H, 2dd, CH_2N), 5.50–5.60 (1 H, m, CHCl), 7.25–7.55 (5 H, m, Ph), 7.84 (1 H, s, 3-H), ~8.70 (1 H, very br s, NH, ex).

Ethyl 1-(2-chloro-2-phenylethyl)-6-oxo-4-pyrrolidin-1-yl-6,7-dihydro-1*H*-pyrazolo[3,4-*b*]pyridine-5-carboxylate 5i. As described for **5a**, from **4** and pyrrolidine (0.14 g, 2 mmol). Recrystallization from 95% ethanol gave **5i** as a white solid (0.37 g, 68%); mp 247–248 °C; (found: C, 61.04; H, 5.78; N, 13.63%. $C_{21}H_{23}ClN_4O_3$ requires C, 60.79; H, 5.59; N, 13.50%); ν_{max} ($CHCl_3$)/cm^{-1} 1708, 1626 and 1574. δ_H (200 MHz; $CDCl_3$; Me_4Si): 1.27 (3 H, t, *J* 7.0, CH_2CH_3), 2.04 (4 H, br s, $2CH_2$ pyrrolidinyl), 3.70 (4 H, br s, $2CH_2N$ pyrrolidinyl), 4.23 (2 H, q, *J* 7.0, CH_2CH_3), 4.75–5.10 (2 H, 2 dd, CH_2N), 5.35–5.50 (1 H, m, CHCl), 7.20–7.50 (5 H, m, Ph), 7.88 (1 H, s, 3-H), ~13.60 (1 H, very br s, NH, ex).

Ethyl 4-anilino-1-(2-chloro-2-phenylethyl)-6-oxo-6,7-dihydro-1*H*-pyrazolo[3,4-*b*]pyridine-5-carboxylate 5j. As described for **5a**, from **4** and aniline (0.19 g, 2 mmol). Recrystallization from 95% ethanol gave **5j** a white solid (0.41 g, 72%); mp 195–196 °C; (found: C, 63.22; H, 5.13; N, 12.63%. $C_{23}H_{21}ClN_4O_3$ requires C, 63.23; H, 4.84; N, 12.82%); ν_{max} ($CHCl_3$)/cm^{-1} 3381, 1647, 1614 and 1579. δ_H (200 MHz; $CDCl_3$; Me_4Si): 1.25 (3 H, t, *J* 6.8, CH_2CH_3), 4.31 (2 H, near q, *J* 7.0, CH_2CH_3), 4.45–4.65 and 4.75–4.95 (2 H, 2 dd, CH_2N), 5.25–5.40 (1 H, m, CHCl), 6.21 (1 H, s, 3-H), 7.10–7.50 (10 H, m, 2 Ph), ~10.30 (1 H, very br s, NH, ex).

Method B: general procedure for the preparation of pyrazolo-[3,4-*b*]pyridones 5c, 5f and 5j. Representative preparation of ethyl 1-(2-chloro-2-phenylethyl)-6-oxo-4-(2-phenylethyl)amino-6,7-dihydro-1*H*-pyrazolo[3,4-*b*]pyridine-5carboxylate 5c. A solution of ethyl 4-chloro-1-(2-chloro-2-phenylethyl)-6-oxo-6,7-dihydro-1*H*-pyrazolo[3,4-*b*]pyridine-5-carboxylate **4** (0.5 g, 1.3 mmol) and 2-phenylethylamine (0.24 g, 2 mmol) in chloroform (10 cm^3) in a closed vessel was heated (oil bath) at 60 °C, with stirring, for 2 h. After cooling, the mixture was diluted with chloroform (40 cm^3), washed with water (2 × 20 cm^3), dried by magnesium sulfate and evaporated *in vacuo*. The solid residue was recrystallized from 95% ethanol to yield the title compound **5c** (0.21 g, 33%).

Ethyl 1-(2-chloro-2-phenylethyl)-4-cyclopropylamino-6-oxo-6,7-dihydro-1*H*-pyrazolo[3,4-*b*]pyridine-5-carboxylate 5f. As described for **5c**, from **4** and cyclopropylamine (0.11 g, 2 mmol). Recrystallization from 95% ethanol gave **5f** (0.31 g, 69%).

Ethyl 4-anilino-1-(2-chloro-2-phenylethyl)-6-oxo-6,7-dihydro-1*H*-pyrazolo[3,4-*b*]pyridine-5-carboxylate 5j. As described for **5a**, from **4** and aniline (0.19 g, 2 mmol). Recrystallization from 95% ethanol gave **5j** (0.09 g, 16%).

Pharmacological assays

Biological methods. Materials. [^{3}H]DPCPX, [^{3}H]CGS 21680 and [^{125}I]AB-MECA were obtained from DuPont-NEN (Boston, MA). Adenosine deaminase was from Sigma Chemical Co. (St. Louis, MO). All other reagents were from standard commercial sources and of the highest commercially available grade.

Receptor binding assays. A_1 and A_{2A} receptor binding. The affinity of the new synthetised compounds towards A_1 and A_{2A} ARs was evaluated by competition experiments assessing their ability to displace [^{3}H]DPCPX and [^{3}H]CGS21680 binding from bovine cortical and striatal membranes, respectively. Binding assays were carried out as previously described.[17–19]

A_3AR binding. Compound affinity towards A_3 ARs were evaluated in membranes obtained from CHO cells transfected with human A_3 AR, kindly supplied by Dr Klotz (Wurzburg, Germany). Competition experiments were performed using [^{125}I]AB-MECA as radioligand following a described procedure[20]

All compounds were routinely dissolved in DMSO and diluted with assay buffer to the final concentration, where the amount of DMSO never exceeded 2%.

At least six different concentrations spanning three orders of magnitude, adjusted appropriately for the IC_{50} of each compound, were used. IC_{50} values, computer-generated using a non-linear regression formula on a computer program (GraphPad, San Diego, CA), were converted to K_i values, knowing the K_d values of radioligands in the different tissues and using the Cheng and Prusoff equation.[21] The dissociation constant (K_d) of [^{3}H]CHA, [^{3}H]CGS 21680, and [^{125}I]AB-MECA were 1.2, 14, and 1.02 nM, respectively.

Computational methods

Data set. For this investigation 65 A_1 AR selective antagonists **6–71** chosen from the literature,[8,22–30] plus a pyrazole[3,4-b]pyridine derivative **62** previously published by us[9] and two of the most interesting compounds among the newly synthesized, namely **5b** and **5g**, were collected. In Table 2 are reported their molecular structures and their affinity value towards the A_1 AR from rat cerebral cortex, expressed as K_i (nM). The reduced availability of affinity data on A_1 agonists for the human A_1 receptor still hampers the study of agonist–receptor interactions in the A_1AR model, this is why we therefore employed a larger dataset of affinity values as determined in rat brain, considering that the sequences of the A_1AR in the two species have a percentage identity of 94.8% and the amino acid differences are located in the TM4–5 loop and in the carboxy-terminal cytoplasmic segment.

Calculations were performed transforming the original affinity in p*K*i and using it as CoMFA dependent variable.

Docking Studies. Molecular structures of ligands **5b** and **5g** and **6–71** were built and energy minimized within MacroModel.[31] Conformational analysis was carried out using the AMBER* force field, as included in MacroModel. For all compounds, the resulting geometries of the lower energy conformers were re-optimized with semi-empirical quantum mechanic calculations, using the Hamiltonian AM1 as implemented in Spartan[32] and atomic charges were calculated.

The theoretical three-dimensional model of the human A_1AR previously published by us[11] was used for a two-step docking protocol. In a first phase, each inhibitor was docked into the active site by means of the FlexX module, as implemented in Sybyl version 6.8[33] with the macromolecule and the ligands being flexible. Preparation of the protein for FlexX requires definition of the binding pocket in terms of "interaction points". In this work the active site was defined as all atoms within a distance of 10 Å from adenosine, the natural substrate, whose binding mode has been defined in ref. 11. This specific distance was determined in order to ensure a significant portion of the active site for the docking experiments. Starting from the best-docked geometries, as obtained with FlexX, the second step consisted in a further refinement of the complex performed with QXP.[34] Also the algorithm implemented in the QXP program allows for fully flexibility of the inhibitors and simultaneous flexibility of the active site side-chains. Each docking run included 15 000 steps

of Monte Carlo perturbation, subsequent fast searching, and final energy minimisation. The results were evaluated in terms of total estimated binding energy, internal strain energy of the ligand, Van der Waals and electrostatic interaction energies and for each ligand, the 20 best docked conformations, according to the QXP score, were saved and analysed further.

CoMFA analysis. The conformers of **14–16**, **35**, **46**, **56**, **64** and **67–71**, selected through the docking procedure described above, were used as templates for all other antagonists in order to elaborate a useful alignment of compounds **6–71**. The DISCO module implemented in Sybyl was used to optimize this superimposition. Compound **15** (KW3902), the most active antagonist among our data set, was selected as template molecule for DISCO calculations.

The aligned molecules were placed one by one in a 3D cubic lattice with 2 Å grid; a methyl probe with a +1 charge was used to calculate steric and electrostatic fields, represented by Van der Waals potential and columbic term, respectively. A 30 Kcal mol^{-1} energy cut-off was applied, which means the steric and electrostatic energies greater than 30 Kcal mol^{-1} are truncated to the value and, thus, can avoid infinity of energy values inside molecule. Regression analyses were performed applying the partial least squares (PLS) algorithm in Sybyl; the steric field alone and the combination of the steric and electrostatic fields were used as structural descriptors to evaluate their correlation with affinity (p*K*i) data. Cross-validations in PLS was used in the meaning of obtaining the optimal number of components to be used in the subsequent analyses. PLS analysis based on least squares fit gave a correlation with a cross-validated r^2_{cv} of 0.540 with a maximum number of components set equal to five. Final CoMFA model was generated using non-cross-validated PLS analysis with the optimum number of components to give an r^2_{cv} 0.937. To obtain statistical confidence limits, the non-cross-validated analysis was repeated with ten bootstrap groups, which yielded an r^2 of 0.960 (optimum number of components was five), SEP = 0.229, std dev = 0.014, steric contribution = 0.510 and electrostatic contribution = 0.490 (Table 4).

In ref. 35 the CoMFA protocol followed is reported in detail.

All calculations were carried out on SGI O2 workstations and on a standard personal computer running under Linux.

Acknowledgements

Financial support from Italian MIUR (Cofin 2002, prot. 2002038577_002) is gratefully acknowledged.

References

1 T. V. Dunwiddie and S. Masino, *Annu. Rev. Neurosci.*, 2001, **24**, 31–55.
2 N. J. Emptage, C. A. Reid and A. Fine, *Neuron*, 2001, **29**, 197–208.
3 T. Takigawa and C. Alzheimer, *J. Physiol.*, 2002, **539**, 67–75.
4 B. B. Fredholm, A. P. Ijzerman, K. A. Jacobson, K.-N Klotz and J. Linden, *Pharmacol. Rev.*, 2001, **53**, 527–552.
5 S. Hess, *Expert Opin. Ther. Pat.*, 2001, **11**, 1533–1561.
6 C. E. Muller, *Expert Opin. Ther. Pat.*, 1997, **7**, 419–440.
7 J. W. Daly, K. D. Hutchinson, S. I. Secunda, D. Shi, W. L. Padgett and M. T. Shamin, *Med. Chem. Res.*, 1994, **4**, 293–306; S. Psychoyos, C. J. Ford and M. A. Phillips, *Biochem. Pharmacol.*, 1982, **31**, 1441–1442.
8 H. W. Hamilton, D. F. Ortwine, D. F. Worth and J. A. Bristol, *J. Med. Chem.*, 1987, **30**, 91–96; S. A. Poulsen and J. R. Quinn, *J. Med. Chem.*, 1996, **39**, 4156–4161.
9 F. Bondavalli, M. Botta, O. Bruno, A. Ciacci, F. Corelli, P. Fossa, A. Lucacchini, F. Manetti, C. Martini, G. Menozzi, L. Mosti, A. Ranise, S. Schenone, A. Tafi and M. L. Trincavelli, *J. Med. Chem.*, 2002, **45**, 4875–4887 and references cited therein.
10 S. Schenone, O. Bruno, F. Bondavalli, A. Ranise, L. Mosti, G. Menozzi, P. Fossa, F. Manetti, L. Morbidelli, L. Trincavelli, C. Martini and A. Lucacchini, *Eur. J. Med. Chem.*, 2004, **2**, 153–160 and references cited therein.
11 F. Giordanetto, P. Fossa, G. Menozzi, S. Schenone, F. Bondavalli, A. Ranise and L. Mosti, *J. Comput.-Aided Mol. Des.*, 2003, **17**, 39–51.
12 A. Bolognese, G. Correale, M. Manfra, A. Lavecchia, E. Novellino and V. Barone, *Org. Biomol. Chem.*, 2004, **2**, 2809–2813 and literature cited therein.
13 T. Y. H. Wu, P. G. Schultz and S. Ding, *Org. Lett.*, 2003, **5**, 3587–3590.
14 R. A. F. de Ligt, P. A. M. van der Klein, J. K. von Frijtag Drabbe Künzel, A. Lorenzen, F. A. El Maate, S. Fujikawa, R. van Westhoven, T. van den Hoven, J. Brussee and A. P. Ijzerman, *Bioorg. Med. Chem.*, 2004, **12**, 139–149.
15 M. Rarey, B. Kramer, T. Lengauer and G. Klebe, *J. Mol. Biol.*, 1996, **261**, 470–489.
16 R. D. Cramer, III, D. E. Patterson and J. D. Bunce, *J. Am. Chem. Soc.*, 1988, **110**, 5959–5967.
17 F. Da Settimo, G. Primofiore, S. Taliani, A. M. Marini, C. La Motta, E. Novellino, G. Greco, A. Lavecchia, L. Trincavelli and C. Martini, *J. Med. Chem.*, 2001, **44**, 316–327.
18 V. Colotta, D. Catarzi, F. Varano, L. Cecchi, G. Filacchioni, C. Martini, L. Trincavelli and A. Lucacchini, *J. Med. Chem.*, 2000, **43**, 1158–1164.
19 I. M. Pirovano, A. P. IJzerman, P. J. M. van Galen and W. Soudijn, *Eur. J. Pharmacol.*, 1989, **172**, 185–193.
20 V. Colotta, D. Catarzi, F. Varano, L. Cecchi, G. Filacchioni, C. Martini, L. Trincavelli and A. Lucacchini A, *J. Med. Chem.*, 2000, **43**, 3118–3124.
21 Y. C. Cheng and W. H. Prusoff, *Biochem. Pharmacol.*, 1973, **22**, 3099–3108.
22 R. H. Erickson, R. N. Hiver, S. W. Feeney, P. R. Blake, W. J. Rzeszotarsky, R. P. Hicks, D. G. Costello and M. E. Abreu, *J. Med. Chem.*, 1991, **34**, 1431–1435.
23 R. F. Bruns, J. H. Fergus, E. W. Badger, J. A. Bristol, L. A. Santay, J. D. Hartman, S. J. Hays and C. C. Huang, *Naunyn-Schmiedeberg's Arch. Pharmacol.*, 1987, **335**, 59–63.
24 H. Nonaka, M. Ichimura, M. Takeda, T. Kanda, J. Shimada, F. Suzuki and H. Kase, *Br. J. Pharmacol.*, 1996, **117**, 1645–1652.
25 C. H. Liu, B. Wang, W. Z. Li, L. H. Yun, Y. Liu, R. B. Su, J. Li and H. Liu, *Bioorg. Med. Chem.*, 2004, **12**, 4701–4707.
26 B. K. Trivedi and R. F. Bruns, *J. Med. Chem.*, 1988, **31**, 1011–1014.
27 V. Colotta, L. Cecchi, D. Catarzi, G. Filacchioni, C. Martini, P. Tacchi and A. Lucacchini, *Eur. J. Med. Chem.*, 1995, **30**, 133–139.
28 R. A. F. De Ligt, P. A. M. Van der Klein, J. K. von Frijag Drabbe Kunzel, A. Lorenzen, F. Ait el Mate, S. Fujikawa, R. van Westhoven, J. Brussee and A. P. Ijzerman, *Bioorg. Med. Chem.*, 2004, **12**, 139–149.
29 P. J. M. van Galen, P. Nissen, I. van Wijngaarden and A. P. Ljzerman, *J. Med. Chem.*, 1991, **34**, 1202–1206.
30 T. Terai, Y. Kita, T. Kusumoki, T. Himazaki, T. Ando, H. Horiai, A. Akamane, Y. Shiokawa and K. Yoshida, *Eur. J. Pharmacol.*, 1995, **279**, 217–225.
31 F. Mohamadi, N. G. J. Richards, W. C. Guida, R. Liskamp, M. Lipton, C. Caufield, G. Chang, T. Hendrickson and W. C. Still, *J. Comput. Chem.*, 1990, **11**, 440–467.
32 Spartan ′02, http://www.wavefun.com.
33 *Sybyl v. 6.8*, TRIPOS Associates, St. Louis, MO.
34 C. McMartin and R. Bohaceck, *J. Comput.-Aided Mol. Des.*, 1997, **11**, 333–344.
35 A. Li, S. Moro, N. Forsyth, N. Melman, X. Ji and K. A. Jacobson, *J. Med. Chem.*, 1999, **42**, 706–721.